the plant journal

SEB SOCIETY FOR EXPERIMENTAL BIOLOGY

The Plant Journal (2021) doi: 10.1111/tpj.15627

CmLHP1 proteins play a key role in plant development and sex determination in melon (*Cucumis melo*)

Natalia Yaneth Rodriguez-Granados[1], Juan Sebastian Ramirez-Prado[2,3], Rim Brik-Chaouche[1], Jing An[1], Deborah Manza-Mianza[1], Sanchari Sircar[1], Christelle Troadec[1], Melissa Hanique[1], Camille Soulard[1], Rafael Costa[1], Catherine Dogimont[4], David Latrasse[1], Cécile Raynaud[1], Adnane Boualem[1], Moussa Benhamed[1] and Abdelhafid Bendahmane[1]*

[1]*Institute of Plant Sciences Paris-Saclay (IPS2), CNRS, INRA, University Paris-Sud, University of Evry, University Paris-Diderot, Sorbonne Paris-Cite, University of Paris-Saclay, Batiment, 630, 91405 Orsay, France,*
[2]*Centre of Microbial and Plant Genetics, KU Leuven, 3001 Leuven, Belgium,*
[3]*VIB Center for Plant Systems Biology, 9052 Ghent, Belgium, and*
[4]*INRA, UR 1052, Unité de Génétique et d'Amélioration des Fruits et Légumes, BP 94, F-84143 Montfavet, France*

Received 4 May 2021; revised 26 November 2021; accepted 9 December 2021.
*For correspondence (e-mail abdelhafid.bendahmane@inra.fr).

SUMMARY

In monoecious melon (*Cucumis melo*), sex is determined by the differential expression of sex determination genes (SDGs) and adoption of sex-specific transcriptional programs. Histone modifications such as H3K27me3 have been previously shown to be a hallmark associated to unisexual flower development in melon; yet, no genetic approaches have been conducted for elucidating the roles of H3K27me3 writers, readers, and erasers in this process. Here we show that melon homologs to Arabidopsis LHP1, CmLHP1A and B, redundantly control several aspects of plant development, including sex expression. *Cmlhp1ab* double mutants displayed an overall loss and redistribution of H3K27me3, leading to a deregulation of genes involved in hormone responses, plant architecture, and flower development. Consequently, double mutants display pleiotropic phenotypes and, interestingly, a general increase of the male:female ratio. We associated this phenomenon with a general deregulation of some hormonal response genes and a local activation of male-promoting SDGs and MADS-box transcription factors. Altogether, these results reveal a novel function for CmLHP1 proteins in maintenance of monoecy and provide novel insights into the polycomb-mediated epigenomic regulation of sex lability in plants.

Keywords: polycomb-mediated gene repression, sex determination, cucurbits, sex allocation, flower development.

INTRODUCTION

Sex determination in plants is the developmental process by which male and female gamete-producing structures are spatially separated along the plant (i.e., monoecious species) or in different individuals (i.e., dioecious species) (Tanurdzic and Banks, 2004). Plant sex determination mechanisms are eclectic, ranging from intrinsically genetic (e.g., evolution of sex chromosomes) to environmental (e.g., temperature, photoperiod, phytohormones, among others) (Pannell, 2017). One of the most relevant characteristics of plant sex determination is the high frequency of species displaying labile sex (Korpelainen, 1998), in which sex allocation – favoring male or female parental functions – constantly changes in response to internal and external factors. This property is commonly found in monoecious species, where sex determination mechanisms are highly sensitive to the environment (Irish and Nelson, 1989). In addition, sexual fate in these species is determined locally at the flower primordia, is often age- and position-dependent, and is controlled by genetic switches that continuously operate during the plant life cycle (Korpelainen, 1998; Pannell, 2017). Such permanent regulation of sex determination genes (SDGs), and the genetic networks they establish, imperatively requires feedback loops that ensure continuous setting and re-setting of the sex determination decision.

Melon (*Cucumis melo*) is an economically important crop widely known for its high diversity in sexual morphs and considered as a model organism for sex determination studies (Grumet and Taft, 2011; Harkess and Leebens-

Mack, 2016; Ma and Pannell, 2016). In several members of the Cucurbitaceae family, including melon, flower primordia are initially bisexual but often undergo sex determination (Grumet and Taft, 2011). During this process, either carpel or stamen primordia are selectively aborted in the developing flower bud, thus leading to the formation of unisexual flowers (Bai and Xu, 2013; Rodriguez-Granados et al., 2017). Sex determination in melon and cucumber (*Cucumis sativus*), its close relative, is regulated by three major SDGs: *CmACS11* and *CmACS7*, which encode two 1-aminocyclopropane-1-carboxylic acid synthases (ACS) involved in the ethylene biosynthetic pathway, and *CmWIP1*, coding for a leucine zipper transcription factor (TF) (Boualem et al., 2008, 2015; Martin et al., 2009).

In monoecious melon and cucumber, coexistence of flowers of opposite sex relies on the differential expression of *CmACS11* and *CmWIP1*, the master SDGs promoting female and male flower development, respectively (Boualem et al., 2015; Martin et al., 2009). In these species, the proportion of male flowers (MFs) and female flowers (FFs) is position-dependent and continuously influenced by several environmental factors such as temperature, photoperiod, and developmental cues, among others (Korpelainen, 1998; Lai et al., 2017, 2018). Under optimal conditions, genetic sex determination (GSD) takes a predominant role and flower sexual fate is determined in a position-dependent manner where FF production is exclusively observed at the most proximal nodes of lateral branches (LBs) (Boualem et al., 2015; Harkess and Leebens-Mack, 2016). This scenario changes under suboptimal conditions where environmental sex determination (ESD) dominates over GSD and leads to changes in sex allocation (e.g., male:female ratio) as an adaptive response (Korpelainen, 1998; Lai et al., 2017, 2018).

In a previous study, we have shown that the acquisition of sex-specific gene expression is regulated at the chromatin level by H3K27me3, a histone mark commonly found in transcriptionally repressed genes. Notably, sex-specific profiles of H3K27me3 were not only observed on hormone-related and flower development genes but also in master SDGs such as *CmWIP1*, thereby suggesting a potential role of H3K27me3 in unisexual flower development (Latrasse et al., 2017).

H3K27me3 is a repressive histone mark with major implications in animal and plant development. This mark is deposited by a subclass of polycomb group (PcG) proteins that interact and form a complex known as polycomb repressive complex 2 (PRC2) (Hennig and Derkacheva, 2009; Reinberg, 2011; Schubert et al., 2006). The catalytic unit of PRC2, also known as the 'writer', deposits H3K27me3 at its genomic targets through the histone methyltransferase activity of the SET domain (Derkacheva and Hennig, 2014). Three PRC2 'writers' have been identified in Arabidopsis: CURLY LEAF (CLF) (Goodrich et al., 1997), SWINGER (SWN) (Chanvivattana et al., 2004), and MEDEA (MEA) (Grossniklaus et al., 1998). While AtCLF and AtSWN play redundant roles in vegetative development and flowering (Chanvivattana et al., 2004), AtMEA controls H3K27me3 deposition during seed development (Köhler et al., 2003).

Downstream molecular events in response to H3K27me3 require the action of the so-called 'readers', which bind H3K27me3 marks and recruit other epigenetic regulators for local chromatin compaction and gene repression (Derkacheva and Hennig, 2014). The plant LIKE HETEROCHROMATIN PROTEIN1 (LHP1) is an H3K27me3 reader in Arabidopsis (Feng and Lu, 2017; Turck et al., 2007; Veluchamy et al., 2016). Despite its structural homology with the *Drosophila* H3K9me2 reader DmHP1 (Gaudin et al., 2001), the LHP1 chromodomain (CD) has a higher affinity for H3K27me3 in facultative heterochromatin (Exner et al., 2009; Libault et al., 2005; Turck et al., 2007). LHP1 acts as a molecular hub, interacting with other proteins and RNA molecules through its chromoshadow domain (CSD) and hinge regions, respectively (Berry et al., 2017; Feng and Lu, 2017; Gaudin et al., 2001; Latrasse et al., 2011). Furthermore, previous studies have revealed additional roles of LHP1 in H3K27me3 maintenance and reinforcement, as PRC2 components can be recruited by LHP1 through mechanisms dependent on and independent of H3K27me3 (Derkacheva and Hennig, 2014; Mylne et al., 2006).

With the purpose of providing genetic evidence for the role of PRC complexes in melon sex determination, we screened for loss-of-function mutations in H3K27me3 writers and readers through Targeting Induced Local Lesions in Genomes (TILLING). The melon genome encodes two H3K27me3 writers, hereafter CmCLF and CmSWN, and two LHP1 homologs (i.e., CmLHP1A and B). Splicing and non-sense mutant alleles of *CmCLF* were recessive lethal whereas those of *CmSWN* did not cause any developmental phenotype, thus suggesting a predominant role of CmCLF in plant development. We also identified a splicing mutation in *CmLHP1A* and a non-sense mutation in *CmLHP1B*. Our results suggest that CmLHP1A and B redundantly control plant development, as severe pleiotropic phenotypes were mainly found in *Cmlhp1ab* double mutants. Interestingly, these plants also display sex allocation changes where the male:female ratio was dramatically increased. In accordance, various genes regulated by H3K27me3 and expressed in a male-specific manner displayed reduced levels of H3K27me3 in *Cmlhp1ab* double mutants, thus leading to their ectopic expression. These include several male-promoting genes such as *CmWIP1*, *CmPI*, and genes involved in auxin homeostasis. Altogether, these results demonstrate that CmLHP1A and B are epigenomic regulators of gene expression with important roles not only in plant development but also in sex determination in melon. Additionally,

this work also provides insights into the roles of these proteins in sex allocation in monoecious species and opens question about the molecular mechanisms behind the well-reported, yet barely explored sex lability in the plant kingdom.

RESULTS

Loss-of-function mutants of PRC components display several defects in plant development

Melon homologs to CLF, SWN, and MEA were identified using PLAZA (Van Bel et al., 2017). In contrast to Arabidopsis, we identified only two putative H3K27me3 methyltransferases, which we named CmCLF (MELO3C020854) and CmSWN (MELO3C017913) based on the protein sequence similarities shared with their Arabidopsis counterparts (Figure S1a). Publicly available RNA sequencing (RNA-seq) data in monoecious melon (Latrasse et al., 2017) showed that both genes are ubiquitously expressed, presenting similar expression levels except for the root, where *CmSWN* transcripts were more abundant (Figure S1b). Annotation of the predicted protein sequences indicated that CmCLF and CmSWN consist of 923 and 890 amino acids (aa), respectively, and retain the SET, Cys-rich, and SANT domains, previously reported for this subfamily in Arabidopsis (Figure S1c) (Huang et al., 2017).

To genetically characterize the functions of *CmCLF* and *CmSWN*, we used the TILLING approach on an ethyl methanesulfonate (EMS) population previously generated for monoecious melon (Dahmani-Mardas et al., 2010). Among the mutations identified, we prioritized the two most deleterious ones (i.e., non-sense and splicing mutations) affecting each gene for further analysis. Therefore, *Cmswn* Q14* (*Cmswn-1*), *Cmswn* Q414*(*Cmswn-2*), *Cmclf* W157* (*Cmclf-1*), and *Cmclf* splicing (*Cmclf-2*) mutants were chosen for phenotyping (Figure S1c).

While *swn* mutants in Arabidopsis do not display major developmental phenotypes (Chanvivattana et al., 2004), *clf* plants are dwarf and early flowering, their leaf blades are curled upwards, and the flowers have several homeotic transformations (Goodrich et al., 1997). Similar to these findings, no major developmental phenotypes were observed in *Cmswn-1* and *Cmswn-2* mutants. Strikingly, we were not able to obtain *Cmclf-1* and *Cmclf-2* homozygous mutants from the M2 segregating population, and *Cmclf* heterozygous plants phenocopied WT individuals, thus suggesting that these *Cmclf* alleles are recessive lethal.

Because of the lethality of *Cmclf* loss-of-function mutants, we decided to elucidate the role of PRC on sex determination by focusing on H3K27me3 readers. We identified two copies of *LHP1* in melon and several members of the Cucurbitaceae family. Each copy clustered into two distinct monophyletic clades, hereafter named groups A and B (Figure 1a). *CmLHP1A* and *CmLHP1B* copies were structurally very similar, both containing the previously annotated CD and CSD (Figure 1b), and predicted to encode proteins of 409 aa and 455 aa, respectively. Although both copies were ubiquitously expressed, as previously observed for the Arabidopsis homolog (Gaudin et al., 2001), the *CmLHP1B* locus displays higher expression levels than *CmLHP1A* in all the analyzed tissues (Figure S2; Latrasse et al., 2017).

Through the TILLING approach, we were able to identify one stop and one splicing mutation in *CmLHP1B* and *CmLHP1A*, respectively. As a common feature, both mutations affect the CSD domain, located at the C-terminal part of the protein. In detail, the *Cmlhp1b* Q409* stop mutation abolishes the last 46 aa of the CSD (Figure 1b,c) while the *Cmlhp1a* splicing mutation leads to the transcription of the last intron (Figure S3). The latter is predicted to result in a frame shift and a protein product of 412 aa, with poorly conserved residues at the C-terminal end of the CSD (Figure 1b,c).

lhp1 mutants in Arabidopsis display a very similar pleiotropic phenotype to the one of *clf* (Gaudin et al., 2001). Conversely, we did not observe major developmental phenotypes in *Cmlhp1a* and *Cmlhp1b* mutants, possibly due to residual protein activity in spite of the mutations and/or functional redundancies between these two paralogs (Figure 2a). To test the latter, we generated and characterized *Cmlhp1ab* double mutants. Interestingly, *Cmlhp1ab* mutants displayed a pleiotropic phenotype characterized by an overall dwarfism, shorter and thinner stems (Figure 2a), smaller curled leaves (Figure 2b), and smaller flowers compared to the WT or any of the single mutants (Figure 2c). We also observed male inflorescences with supernumerary flowers (Figure 2d–f), exceeding the five to eight flower fascicles commonly found in melon (Figure 2e; Rattan and Kumar, 2016). Besides, *Cmlhp1ab* adult plants showed reduced apical dominance and generally disorganized plant architecture (Figure 2g). Altogether, these results are consistent with the known role of LHP1 in plant development and provide evidence for its conservation in the plant kingdom. It is noteworthy that although our genetic approach suggests a functional redundancy between CmLHP1A and B, the extent of this should be addressed in better detail.

CmLHP1A and B positively regulate female flower development and maintenance of monoecy

In monoecious melon, MFs and FFs develop in a position-dependent manner. MFs develop at the main stem (MS) and distal nodes of LBs, whereas FFs are exclusively formed at proximal nodes of LBs (Boualem et al., 2015). H3K27me3 was previously shown as a key repressive histone modification involved in the development of

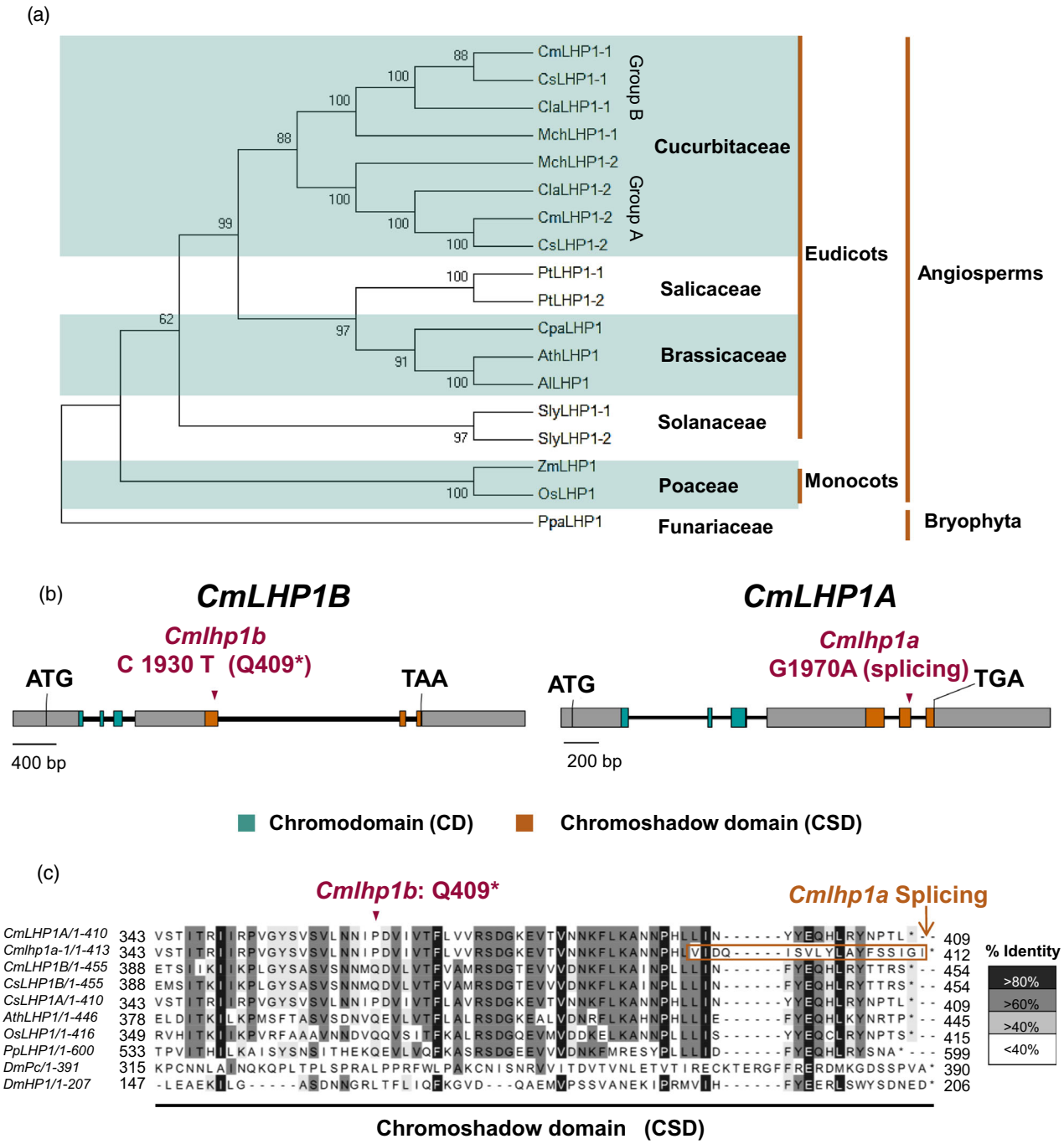

Figure 1. CmLHP1A and B phylogenetic relationships, gene body structures, and protein sequences. (a) Phylogenetic analyses of LHP1 homologs. Protein sequences from different plant species were aligned and used to generate a neighbor-joining phylogenetic tree with 1000 bootstrap replicates. The percentage of replicate trees in which the associated taxa clustered together in the bootstrap test is shown next to the branches. Cs (*Cucumis sativus*), Cm (*Cucumis melo*), Cla (*Citrullus lanatus*), Mc (*Momordica charantia*), Pt (*Populus trichocarpa*), Ath (*Arabidopsis thaliana*), Al (*Arabidopsis lyrata*), Cpa (*Carica papaya*), Sl (*Solanum lycopersicum*), Zm (*Zea mays*), Os (*Oryza sativa*), *Pp* (*Physcomitrella patens*). (b) Gene body structures of *CmLHP1A* and *B*. Gray boxes and black lines correspond to exons and introns, respectively. Gene position of both the chromodomain (CD) and the chromoshadow domain (CSD) are shown. EMS-derived mutations for *CmLHP1A* and *CmLHP1B* are indicated with arrowheads. (c) Protein sequence alignment of the LHP1 CSD. *Cmlhp1b* stop and *Cmlhp1a* splicing mutations are indicated in red and orange, respectively. Protein sequence of the *Cmlhp1a* splicing mutant was included in the alignment and mistranslated residues are shown (orange box). *Drosophila melanogaster* polycomb (DmPc) and HETEROCHROMATIN PROTEIN 1 (DmHP1) are also included in the alignment.

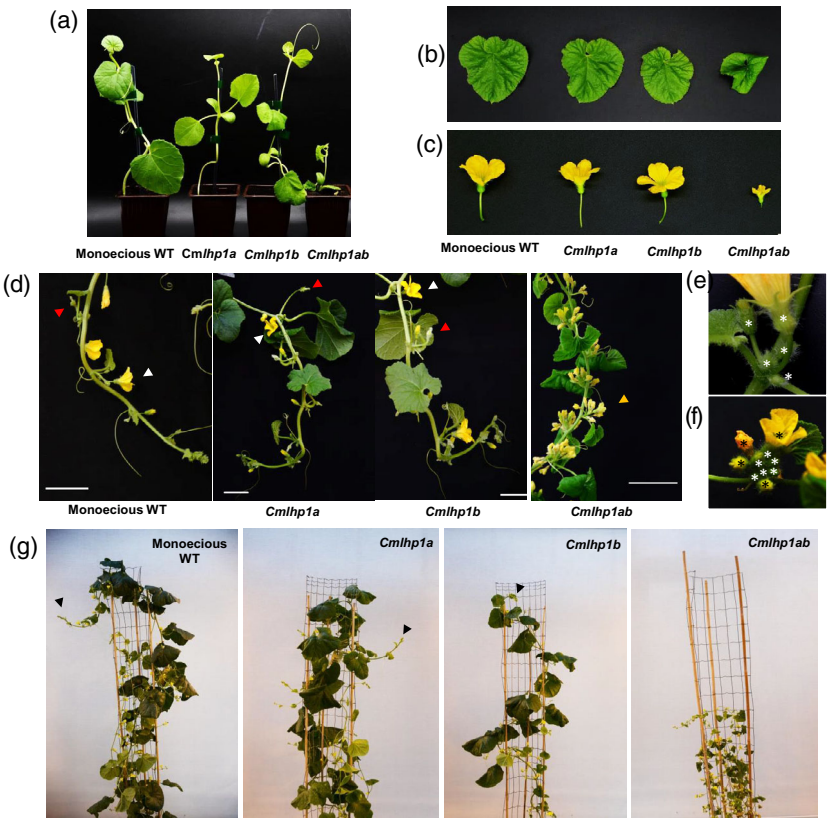

Figure 2. *Cmlhp1ab* double mutants display a pleiotropic phenotype in melon. (a) Two-week-old monoecious WT, *Cmlhp1a*, *Cmlhp1b*, and *Cmlhp1ab* plants. (b) Leaves from adult plants showing a curly leaf phenotype in *Cmlhp1ab*. (c) Male flowers from 2-month-old plants. (d) Secondary branches of adult plants. Normal expression of monoecy is observed in *Cmlhp1a* and *b* and monoecious WT plants, where female flowers (red arrows) develop at the proximal nodes of emerging branches and male flowers (white arrows) develop at distal nodes. This pattern is lost in the *Cmlhp1ab* double mutant, where fewer branches and more supernumerary male inflorescences are observed. Scale bar, 4 cm. (e, f) Male flower fascicles on the main stem (MS) of monoecious WT (e) and *Cmlhp1ab* (f). Flower buds are indicated by asterisks. (g) Two-month-old plants. MSs are easily recognized in *Cmlhp1a* and *b* and monoecious WT plants (black arrows). *Cmlhp1ab* double mutants, in contrast, display an increased branching that leads to an overall distortion of plant architecture.

unisexual flowers and maintenance of monoecy in melon (Latrasse et al., 2017). To assess whether *Cmlhp1ab* mutations could have an impact on sex determination, we looked for sexual transitions (e.g., male-to-female transitions) in *Cmlhp1ab*, *Cmlhp1a*, and *Cmlhp1b* mutants. For this purpose, we focused on the sexual phenotype of flowers derived from the most proximal node of the LBs, hereafter L1, where FFs should develop (Figure 3i). No significant sexual transition was observed in *Cmlhp1a* and *b* single mutants compared to WT plants (Figure 3a–c). In contrast, *Cmlhp1ab* double mutants displayed several sex expression alterations that led to a general shift towards maleness. For instance, some L1 nodes bore FFs, some MFs and FFs simultaneously, and others displayed a total masculinization of the node (Figure 3d–g). We also observed the terminal flower phenotype, traditionally attributed to the *lhp1* mutant in Arabidopsis (Larsson et al., 1998), and that in this case consisted of supernumerary inflorescences of MFs (TMF, Figure 3f). Quantification of male-to-female transitions at L1 nodes showed that *Cmlhp1ab* displays a strong, almost total transition of FFs into MFs (Figure 3h,i). In conclusion, our findings provide genetic evidence for the previously suggested role of H3K27me3 in the maintenance of monoecy in melon and highlights the function of CmLHP1A and B as positive regulators of FF development.

CmLHP1A and B regulate gene expression through the control of H3K27me levels

In order to elucidate the molecular events related to the pleiotropic phenotype observed in *Cmlhp1ab*, we generated RNA-seq data from this mutant and monoecious WT leaves. We decided to work with leaves as it is a more homogenous, convenient tissue for comparative genome-wide analyses. Differential expression analysis detected 2537 deregulated genes in the double mutant, with a higher proportion being upregulated than downregulated (1534 versus 1002 genes) (Figure S4, Data S1). On the one hand, the upregulated gene set was enriched for GO terms related to the development of branching structures, vegetative-to-reproductive transition, and responses to auxin, gibberellin, and ethylene (Figure S2a). On the other hand, downregulated genes, which mainly represent indirect targets, were enriched in GO terms related to the cell cycle, specifically DNA replication and cell division, and plant growth architecture (Figure S4b).

Considering the role of LHP1 in H3K27me3 spreading at PRC2 genomic targets (Derkacheva et al., 2013; Veluchamy et al., 2016), we hypothesized that the observed deregulation of gene expression in *Cmlhp1ab* mutants might be a consequence of genome-wide changes in H3K27me3. To assess this, we first generated H3K27me3 ChIP-seq data

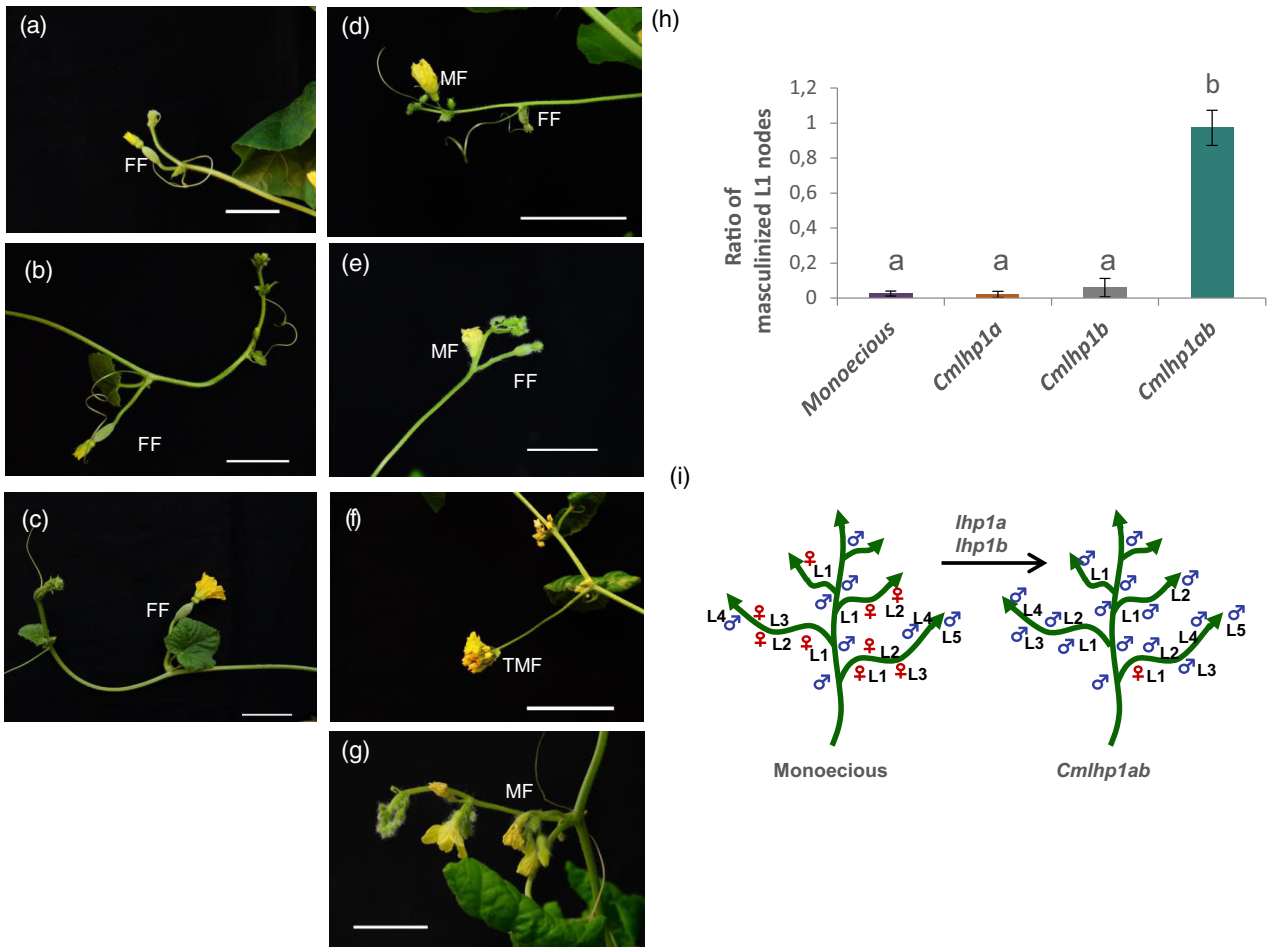

Figure 3. *Cmlhp1ab* double mutants display changes in sex expression. (a–c) Lateral branches bearing female flowers (FFs) in monoecious WT (a), *Cmlhp1a* (b), and *Cmlhp1b* (c). (d–g) Lateral branches of *Cmlhp1ab* bearing an FF (d), flowers of opposite sex at the same node (e), terminal male flowers (TMFs) (f), and branches with MFs (g). (h) Quantification of masculinized nodes. The ratio of L1 nodes bearing male flowers was calculated for monoecious WT, *Cmlhp1a*, *Cmlhp1a*, and *Cmlhp1ab*. Letters represent different statistical groups; $P \leq 0.05$, *t*-test. (i) Graphic representation of *Cmlhp1ab* sex expression phenotype. Scale bars, 2 cm.

from leaves of WT plants. Two biological replicates were processed and found to have a correlation coefficient of at least 0.97 (Figure S5a). The H3K27me3 peak position was determined at the genome-wide level and assigned to the closest coding sequence (CDS). As expected, a strong correlation of the H3K27me3 peak position was observed between both WT datasets. H3K27me3 localized preferentially along the gene body, followed by the gene-flanking regions, where a stronger peak density was observed at the 'distal' promoter region (−5 kb) than at regions downstream the 3′ end of genes (Figure S6a).

We also performed chromatin immunoprecipitation coupled with sequencing (ChIP-seq) analysis against RNA polymerase II (RNAPII), which denotes active transcription, and compared the localization of RNAPII peaks with the ones previously called for H3K27me3. This comparison showed that RNAPII peaks occupy mainly the transcription start sites (TSSs) of genes and poorly colocalize with H3K27me3, consistent with the well-known anticorrelation between H3K27me3 and gene expression (Figure S6b). This was further confirmed after integrating RNA-seq and ChIP-seq data from WT plants, as the lowliest expressed genes displayed the highest intensity of H3K27me3 and *vice versa* (Figure S6c).

We then assessed the relationship between gene expression deregulation in *Cmlhp1ab* and H3K27me3. For this purpose, we first determined the proportion of up- and downregulated genes in *Cmlhp1ab* that are marked by H3K27me3. We found a greater proportion of genes being upregulated and marked by H3K27me3 (905 out of 1534 genes, 59%) than downregulated (367 out of 1002 genes) (Figure 4a). Plotting the levels of H3K27me3 of these 905 and 367 genes revealed that the degree of histone methylation varies greatly between these two sets. Upregulated genes showed higher H3K27me3 levels than downregulated genes (Figure 4b; Figure S6d), thus indicating that

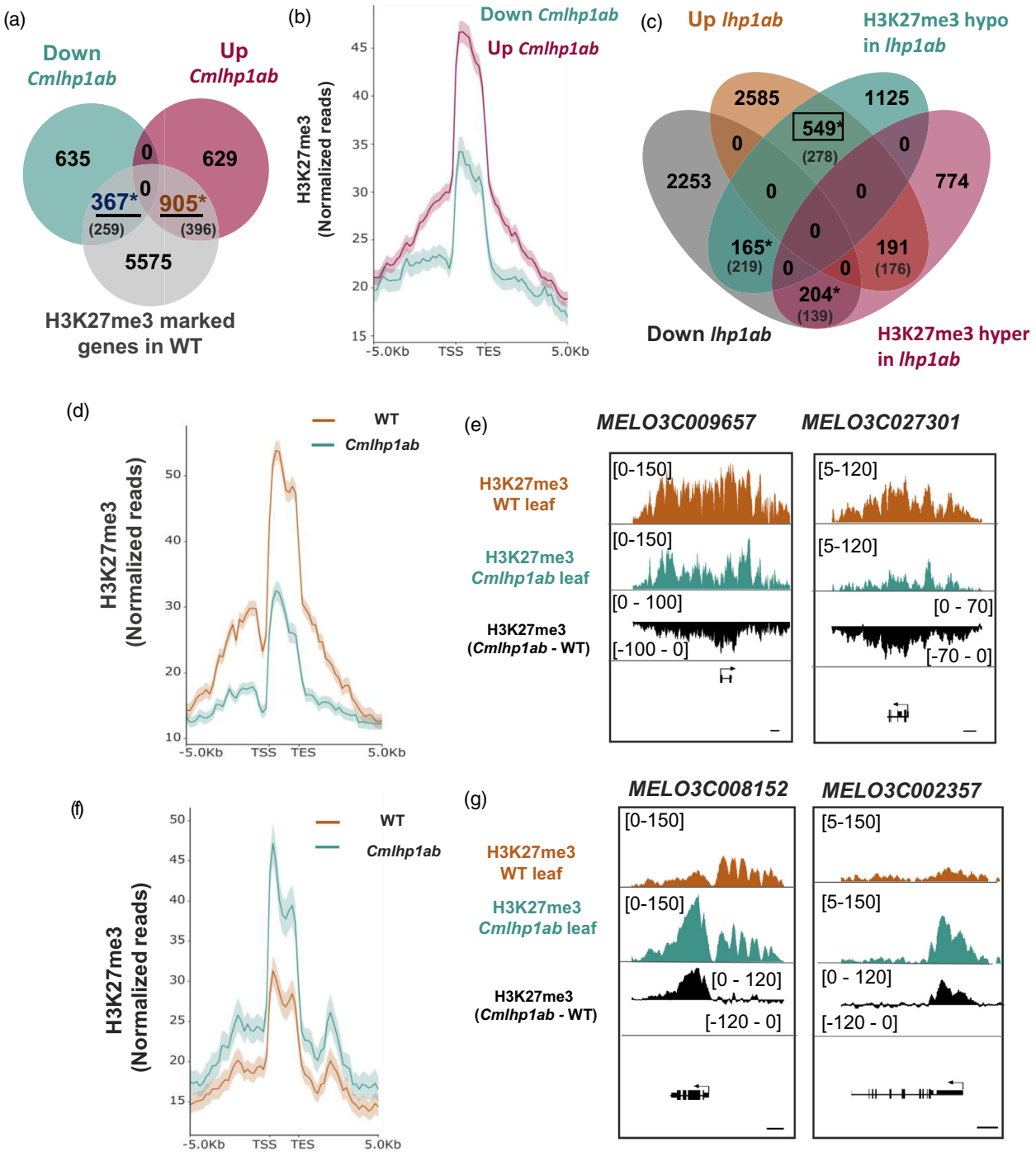

Figure 4. H3K27me3 maintenance and distribution is altered in *Cmlhp1ab* mutants. (a) Venn diagram showing the overlap between H3K27me3-marked genes and deregulated genes in *Cmlhp1ab* mutants. Numbers of overlapping genes expected by chance are shown in parentheses (RNA-seq: $\log_2(FC) \leq -2$ [down] and ≥ 2 [up], $P \leq 0.05$). *$P < 0.005$, Chi-square test. (b) Metaplot showing H3K27me3 normalized read densities (in WT monoecious plants) of up- and downregulated genes in *Cmlhp1ab* (RNA-seq: $\log_2(FC) \leq -2$ [down] and ≥ 2 [up], $P \leq 0.05$). Mean, normalized H3K27me3 reads of equal bins were plotted across a 10-kb window around the transcription start site (TSS) and transcription end site (TES). (c) Venn diagram showing the overlap between H3K27me3 hypo- and hypermethylation and gene expression changes in *Cmlhp1ab* mutants. Numbers of overlapping genes expected by chance are shown in parentheses (RNA-seq: $\log_2(FC) \leq -1$ [down] and ≥ 1 [up], $P \leq 0.05$; ChIP-seq: $\log_2(FC) \leq -0.4$ [hypo] and ≥ 0.4 [hyper], $P \leq 0.05$). *$P < 0.01$, Chi-square test. (d) Metaplot showing H3K27me3 normalized read densities of upregulated and hypomethylated genes (549 genes from panel (c)). (e) Examples of H3K27me3 hypomethylation profiles of two upregulated genes in *Cmlhp1ab*. H3K27me3 levels in WT and *Cmlhp1ab* are shown in orange and blue, respectively. Differences in H3K27me3 levels between WT and mutant (mutant − WT) are shown in black. Scale bar, 2 kb. (f) Metaplot showing H3K27me3 normalized read densities of downregulated and hypermethylated genes (204 genes from panel (c)). (g) Examples of H3K27me3 hypermethylation profiles of two downregulated genes in *Cmlhp1ab*. H3K27me3 levels between WT and mutant (mutant − WT) are illustrated in the subtraction track colored in black. Scale bar, 500 bp.

the differential transcriptional state of these genes might be partly controlled by H3K27me3.

In order to determine if gene deregulation in *Cmlhp1ab* is associated with H3K27me3 changes, we generated two biological replicates of H3K27me3 ChIP-seq on the double mutant and compared them to those from WT plants (Figure S5). A total of 3008 differentially methylated genes were identified in *Cmlhp1ab* (Data S2). Among these, 61% corresponded to hypomethylated genes (1839 out of 3008 genes), in agreement with the positive role of LHP1 in H3K27me3 deposition. Interestingly, we observed that *Cmlhp1ab* mutations also led to hypermethylation of several genes, although they represented a smaller fraction (1169 genes out of 3008, approximately 39%). To address the impact of these changes on gene expression, we compared the lists of deregulated (RNA-seq: $|\log_2(FC)| \geq 1$, $P < 0.05$) and differentially methylated genes of *Cmlhp1ab*. According to this comparison, H3K27me3 hypomethylation was significantly associated with upregulation while hypermethylation was more related to downregulation ($P <$ 1e−6, Chi-square test) (Figure 4c).

LHP1 in Arabidopsis promotes the spreading of H3K27me3 towards the 3′ end of its target genes (Derkacheva et al., 2013; Veluchamy et al., 2016). To evaluate if the H3K27me3 distribution changes in *Cmlhp1ab*, we plotted the H3K27me3 read density of hypo-up (hypomethylated and upregulated) and hyper-down (hypermethylated and downregulated) genes in WT and mutant contexts. Contrary to *lhp1* mutants in Arabidopsis, we observed that H3K27me3 hypomethylation of hypo-up genes in *Cmlhp1ab* is not restricted to the 3′ end of genes, and it can be observed along the gene body and its flanking regions (Figure 4d,e; Figure S7a). This pattern changes in hyper-down genes, for which H3K27me3 hypermethylation is preferentially observed at the gene body (Figure 4f,g; Figure S7b). Altogether, our analyses indicate that CmLHP1 controls H3K27me3 deposition and/or maintenance, and thereby modulates gene expression.

Female-to-male transition in *Cmlhp1ab* mutants is related to male-like expression of master SDGs

Flower sexual fate in monoecious melon is determined by the differential expression of the master SDGs, *CmACS11* and *CmWIP1*. *CmACS11* is expressed in future FFs, where it represses *CmWIP1* and directly activates *CmACS7*, which are the negative regulators of carpel and stamen differentiation, respectively. In MFs, conversely, *CmACS11* is repressed, and *CmWIP1* transcription burst results in carpel arrest and inhibition of *CmACS-7* (Boualem et al., 2015). Expression of these three SDGs was measured in WT and *Cmlhp1ab* flowers collected from the MS (MF in WT and MF in *Cmlhp1ab*) and L1 positions (FF in WT and transitioned-MF in *Cmlhp1ab*) (Figure 3i; Figure S8a). *Cmlhp1ab* flowers – both at the L1 and MS – presented almost undetectable expression of *CmACS7* and *CmACS11*, thus resembling WT MFs and significantly differing from FFs where both genes are upregulated. Similarly, L1- and MS-derived flowers in *Cmlhp1ab* displayed comparable *CmWIP1* expression levels to those of WT MFs (Figure S8a). In order to discern whether these expression patterns are related to H3K27me3 changes in *Cmlhp1ab*, we assessed the distribution of H3K27me3 along *CmACS11*, *CmWIP1*, and *CmACS7* gene bodies. To this end, we used our previous, publicly available H3K27me3 ChIP-seq data from MFs and FFs of monoecious melon (Latrasse et al., 2017), and the ChIP-seq data we generated for *Cmlhp1ab* and WT leaves. H3K27me3 was observed along the gene bodies and flanking regions of these three SDGs in all the tissues analyzed. In comparison to *CmACS11* and *CmACS7*, *CmWIP1* presented the most contrasting profile of H3K27me3 between sexes, with MFs displaying hypomethylation at these loci compared to the FFs. Additionally, *CmWIP1* presented the highest hypomethylation in the *Cmlhp1ab* background, whereas *CmACS11* and *CmACS7* were slightly hypermethylated (Figure S8b).

As a whole, these results indicate that *Cmlhp1ab* female-to-male transition is related to the local acquisition of male-like expression profiles of *CmWIP1*, *CmACS11*, and *CmACS7*. While H3K27me3 hypomethylation could be one explanation for *CmWIP1* expression in *Cmlhp1ab* L1 flowers, it is unclear whether changes in histone methylation are responsible for downregulation of *CmACS11* and *CmACS7*. In agreement with the role of CmLHP1A and B as epigenomic regulators, it is very likely that both proteins control the sex determination pathway through mechanisms that act either upstream or downstream of *CmACS-11*.

CmLHP1A and B control femaleness through H3K27me3-mediated expression of genes involved in flower development and hormone homeostasis

Gene Ontology (GO) analysis of H3K27me3 hypomethylated and upregulated genes in *Cmlhp1ab* showed an enrichment in genes related to flower development and hormone responses (Figure 5a). In a previous study, we identified MF- and FF-specific genes, based on their expression and H3K27me3 levels in FF versus MF (Latrasse et al., 2017). By MF-specific genes we refer to the genes that are hypermethylated and downregulated in FFs, and by FF-specific genes we refer to those that are hypomethylated and upregulated in FFs.

Aiming to elucidate additional molecular events related to the sex expression changes of *Cmlhp1ab*, we crossed MF- and FF-specific gene lists with those of H3K27me3 hypo- and hypermethylated in *Cmlhp1ab*. Through this comparison, we found that 17% (49/275) of FF- and 18% of MF-specific genes (56/304 genes) were hypomethylated in *Cmlhp1ab* mutants (Figure 5b, Data S3).

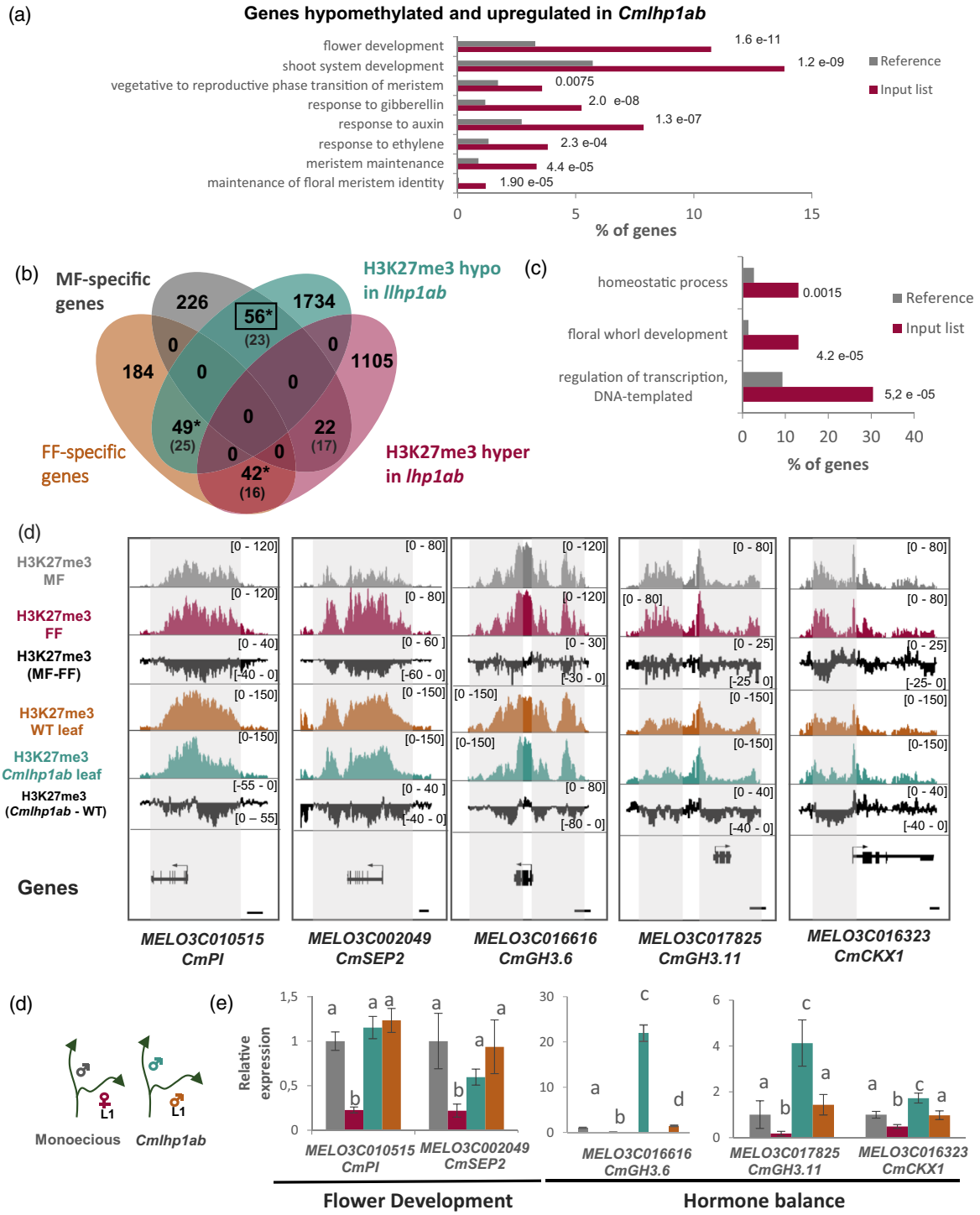

Figure 5. CmLHP1A and B control genes involved in flower development and sex determination via H3K27me3. (a) GO enrichment analyses for biological processes of hypomethylated upregulated genes in *Cmlhp1ab*. (b) Venn diagram representing the overlap between the female flower (FF)- and male flower (MF)-specific genes regulated by H3K27me3 (retrieved from Latrasse et al., 2017) and H3K27me3 changes in *Cmlhp1ab* (ChIP-seq: $\log_2$(FC) cut-off = 0.4, $P \leq 0.05$). Numbers of overlapping genes expected by chance are shown in parentheses. (b) GO terms significantly enriched in FF-specific genes hypomethylated in *Cmlhp1ab* (56 genes from panel (b)). *$P < 0.01$, Chi-square test. (c) H3K27me3 levels in some FF-specific genes hypomethylated in *Cmlhp1ab*. H3K27me3 levels in MF (gray), FF (red) (retrieved from Latrasse et al., 2017), and leaves from WT (orange) and *Cmlhp1ab* (blue) are shown. The differences in H3K27me3 levels between FF and MF (MF − FF) and between WT monoecious and *Cmlhp1ab* leaves are illustrated in black. H3K27me3 hypomethylated regions are highlighted in beige. Scale bar, 2 kb. (d) Schematic representation of WT and *Cmlhp1ab* flowers sampled for gene expression analyses. (e) Expression levels of some MADS-box TFs and hormone homeostasis genes in WT male (gray), female (red), and *Cmlhp1ab* flowers from the main stem (MS, blue)- and the first lateral node (L1)-derived flowers (orange). Letters represent different statistical groups ($P \leq 0.05$, *t*-test). Relative expression was normalized to WT male values.

Considering that FF development in melon results from the repression of male-promoting and female suppressor genes (Diggle et al., 2011; Pannell, 2017), we hypothesized that female-to-male transition in *Cmlhp1ab* could be related to H3K27me3 hypomethylation and ectopic expression of MF-specific genes in flowers at the L1. For this reason, we decided to focus on the 56 MF-specific genes that showed hypomethylation in *Cmlhp1ab*. GO analysis on this gene set showed an enrichment in biological processes such as regulation of transcription, auxin homeostasis, and flower development (Figure 5c). Within this set, we identified TFs such as *CmWIP1* as well as melon homologs to *PISTILLATA* (*PI*) and *SEPALLATA 2* (*SEP2*) of the MADS-box family. In addition, we found enzymatic regulators of auxin and cytokinin responses, including two homologs to the indole-3-acetic acid (IAA)-amido synthetases from the Gretchen Hagen3 (GH3) family (GH3.6 and 3.11-like enzymes) and a cytokinin dehydrogenase (homologous to AtCKX1) (Figure 5d). Expression of the above-mentioned genes was quantified in *Cmlhp1ab* and WT flowers. While MADS-box TF genes, *CmPI* and *CmSEP2*, displayed similar expression levels in *Cmlhp1ab* and WT MFs, we observed that *CmGH3.6*, *CmGH3.11*, and *CmCKX1* were predominantly upregulated in mutant MFs at the MS (Figure 5e), thus suggesting that deregulation of hormone responses might be involved in the sexual phenotype we observed in *Cmlhp1ab* mutants. Altogether, these findings indicate that CmLHP1A and B are necessary for repressing MF-specific genes in FFs and for controlling their expression in a position-dependent manner.

DISCUSSION

Conserved protein structure and roles of PcG proteins in plant development

Plant homologs to Enhancer of Zeste [E(z)], the H3K27me3 writer in *Drosophila*, have undergone several duplication events within the plant kingdom. Evolutionary studies have shown that CLF is the ancestral H3K27me3 writer in plants while SWN emerged in angiosperms, and MEA resulted from a gene duplication event specific to the Brassicaceae family (Huang et al., 2017; Qiu et al., 2017). Congruent with these findings, we showed that the melon genome encodes two H3K27me3 writers, which share a higher similarity to CLF and SWN than MEA.

CLF and SWN play redundant roles in Arabidopsis, a fact that is often related to the ubiquitous expression patterns of these two proteins (Lafos et al., 2011; Qiu et al., 2017). Similarly, *CmCLF* and *CmSWN* expression did not show major tissue specificities, thus suggesting a functional redundancy between them (Qiu et al., 2017, Figure S1b). Our genetic study, however, suggests that CmCLF plays a predominant role in plant development instead of functioning redundantly with CmSWN. Considering the lethality of the *Cmclf* mutants analyzed in this work, less deleterious alleles are necessary to characterize the function of CLF in melon.

Homologs of LHP1 have been identified in several plant families (Chen et al., 2016). In this study, we identified two different orthologs in several cucurbits, including melon. *CmLHP1A* and *B* displayed constitutive, yet different expression levels across several tissues, suggesting that they are subject to different regulatory mechanisms. Although our results support functional redundancy between CmLHP1A and B, it is possible that the mutations analyzed here are not severe enough to notice major developmental phenotypes in *Cmlhp1a* and *Cmlhp1b* single mutants. Despite this, we observed pleiotropic phenotypes in *Cmlhp1ab* double mutants that closely resemble those observed in Arabidopsis and moss (*Physcomitrella patens*), indicating that LHP1's role in plant development is conserved across different taxa (Gaudin et al., 2001; Parihar et al., 2019). Remarkably, *Cmlhp1ab* mutants also displayed an increase in the male:female ratio, which indicates that LHP1 not only controls overall plant development but also specific developmental processes such as sex determination.

LHP1 controls developmental processes in *C. melo* through the regulation of H3K27me3 levels and distribution

At the transcriptomic level, *Cmlhp1ab* mutants displayed deregulation of multiple genes, with a major impact on gene upregulation. Although this finding agrees with the reported role of LHP1 as a transcriptional repressor, our data also highlighted a substantial number of upregulated genes. We consider that gene upregulation corresponds mainly to indirect effects, which have been commonly observed in previous studies (Feng and Lu, 2017; Piacentini et al., 2003; Rizzardi et al., 2011; Wei et al., 2017).

Most importantly, we observed that the changes in transcription in *Cmlhp1ab* are coherent with the pleiotropic phenotype we observed. Overall reduced growth and curly leaf phenotypes could be explained by the downregulation of genes controlling the cell cycle (Figure S4b). Indeed, LHP1 has been shown to play a role in the maintenance of the epigenetic memory during DNA replication by interacting with two different DNA polymerase subunits, the DNA polymerase α subunit INCURVATA2 (ICU2) (Barrero et al., 2007) and the DNA polymerase ε subunit EARLY IN SHORT DAYS 7 (ESD7) (Del Olmo et al., 2010). In addition, LHP1 in Arabidopsis interacts with CYCLOPHILIN71 (CYP71) and can also form a complex with ASYMMETRIC LEAVES1 (AS1) and AS2 to control leaf development and differentiation (Li et al., 2016). Similarly, altered plant architecture in *Cmlhp1ab* mutants could be a consequence of the upregulation of genes involved in hormone responses, branching, and flower and shoot development (Figure S4a).

In general, H3K27me3 was negatively correlated to RNA-PII occupancy on genes (Figure S6b), suggesting that in most cases both elements are exclusive. This result is also coherent with the known repressive role of H3K27me3 in transcription, which was confirmed by assessing the relation between H3K27me3 and gene expression levels (Figure S6c).

The role of LHP1 in the maintenance of H3K27me3 was confirmed by the high proportion of genes that turned hypomethylated in *Cmlhp1ab*. Consistent with preceding studies, mutations in LHP1 can also lead to histone hypermethylation (Veluchamy et al., 2016), possibly due to the deregulation of other H3K27me3 erasers and/or writers. Besides, hypermethylated genes in *Cmlhp1ab* exhibited low levels of H3K27me3 in the WT context (Figure 4b; Figure S6d), thus supporting a role of this protein not only in promotion H3K27me3 accumulation, but also in the control of its homeostasis and genomic distribution. Our results equally indicate that CmLHP1 controls the spatial occupancy of H3K27me3 along the gene body and flanking regions. This fact suggests that CmLHP1's recruitment might precede H3K27me3 or that it is strongly necessary for H3K27me3 deposition at many loci. In Arabidopsis, for instance, LHP1 can be recruited in a PRC2-independent manner by TFs such as SHORT VEGETATIVE PHASE (SVP) for *SEP3* repression or by PRC1-mediated recruitment (Derkacheva and Hennig, 2014; Liu et al., 2009). These results highlight the complex relationship of PRC1- and PRC2-dependent as well as -independent mechanisms for H3K27me3 deposition and gene repression, with LHP1 acting as a molecular bridge. Finally, we also showed that H3K27me3 changes in *Cmlhp1ab* can have an impact on gene expression and that hypomethylation is more strongly associated with gene upregulation.

LHP1 mediates gene repression of genes involved in sex determination and flower development

Sex determination in cucurbits and other species have a well-defined genetic component. In the case of melon and cucumber, GSD in monoecious species is primarily regulated by a genetic switch operating on *CmACS11* and *CmWIP1* (Boualem et al., 2008; Pannell, 2017). *CmACS11* and *CmWIP1* gain- and loss-of-function mutations have been repeatedly selected over time and considered as main events in the evolution of sexual systems in cucurbits (Boualem et al., 2015). It has been previously demonstrated that the emergence of gynoecy in melon is associated with the insertion of the *Gyno-HAT* transposon nearby *CmWIP1*. *Gyno-HAT* is exclusively present in gynoecious lines and shown to permanently repress *CmWIP1* for total feminization (Martin et al., 2009). The role of DNA methylation in sex determination is not specific to cucurbits and extends to other families (Akagi et al., 2016; Chuck et al., 2007; Li et al., 2021; Vyskot et al., 1993). Chromatin modifications are well known for their reversibility, a property conferred by the action of writers, readers, and erasers. It is therefore reasonable to expect a role of histone modifications in the control of SDGs, especially in monoecious species where sex is labile and spatiotemporally regulated. Consistently, we previously showed that H3K27me3 is deposited on the *CmWIP1* locus and that this deposition is CmACS11-dependent (Latrasse et al., 2017). *Cmlhp1ab* mutants, which considerably phenocopy *Cmacs11*, provide genetic evidence for this. Moreover, *CmWIP1* is hypomethylated in *Cmlhp1ab* mutants (Figure S8b), which suggests H3K27me3 could function as a dynamic regulatory mechanism of SDG expression. Future research needs to be conducted to determine whether this mechanism is responsive to different environmental conditions.

Hypomethylated-upregulated genes in *Cmlhp1ab* were enriched for GO terms related to flower development and hormone responses (Figure 5a). Consistently, previous studies have reported that LHP1 participates in the regulation of auxin (Ariel et al., 2016), ethylene (Hu et al., 2011), abscisic acid (Ramirez-Prado et al., 2019), and gibberellin responses in Arabidopsis (Cui and Benfey, 2009). Interestingly, LHP1 is also a major regulator of several homeotic genes, including *SEP2*, *SEP3*, *SHATTERPROOF1* (*SHP1*), and *SHP2*, all of them typically related to floral meristem differentiation and flower development (Kotake et al., 2003; Turck et al., 2007).

With the purpose of elucidating the molecular events related to the sexual phenotype of *Cmlhp1ab* mutants, we identified the MF- and FF-specific genes that display H3K27me3 changes in *Cmlhp1ab*, using the dataset we generated on leaves. For this, we assumed that H3K27me3 in these mutants is globally affected across tissues. We are aware that this comparison might represent a caveat if one intends to identify all the genes regulated by LHP1 in the context of sex determination and this needs to be considered for future studies. Despite of this limitation, we were able to pick out potential MF-specific genes that are deregulated in *Cmlhp1ab* mutants and that could be related to the sex expression changes we observed.

MADS-box TFs belonging to the B- and C-classes play a key role in determining stamen and carpel identities, respectively (Coen and Meyerowitz, 1991). In addition, the expression of these genes is maintained even after sex determination and their differential expression is associated with the production of unisexual flowers (Pfent et al., 2005; Sather et al., 2010; Yang et al., 2019). This indicates that MADS-box TFs are not only required for floral whorl identity, but also that they can be directly or indirectly controlled by SDGs for organ differentiation. Our results showed that *CmPI* (encoding a B-class MADS-box TF) and *CmSEP2* (encoding an E-class MADS-box TF) are controlled by H3K27me3 and that CmLHP1 is required for

reinforcing this mark (Figure 5d). MADS-box TF genes such as *AG*, *PI*, and *SEP3* are also common PRC2 targets in Arabidopsis (Schubert et al., 2006; Veluchamy et al., 2016).

In cucumber, exogenous treatment with auxin and cytokinin results in an increase of femaleness, as both hormones induce ethylene synthesis and signaling (Galun, 1959; Pawełkowicz et al., 2019b; Takahashi et al., 1980). We observed that homologs to AtGH3 and AtCKX1 enzymes, which are involved in IAA activation and cytokinin degradation, respectively, are expressed in the WT MF, as previously reported in cucumber (Pawełkowicz et al., 2019a). Furthermore, these genes become significantly upregulated in the MS-derived flowers of *Cmlhp1ab*, thus suggesting that they can be spatially controlled by PRC2. Accordingly, previous studies have reported that some members of the CKX and GH3 families are repressed through H3K27me3 deposition in Arabidopsis and rice (*Oryza sativa*) (He et al., 2012; Liu et al., 2015). These findings suggest that auxin and cytokinin in the nodes of the MS might play a role in the establishment of the position identity of young LBs and therefore the development of FFs at L1.

We observed that *Cmlhp1ab* mutations impacted, to a greater extent, the expression of hormone homeostasis genes in flowers at the MS. Conversely, these mutations do not seem to significantly affect the expression of *CmPI*, *CmSEP2*, and male-promoting SDGs in either L1- or MS-derived flowers (Figure 6d). These findings suggest that hormonal imbalance may be the predominant endogenous cue affecting flowers at the MS and that this alteration impacts the sexual fate of L1-derived flowers. In addition, for this reason, we conclude that female-to-male transition in *Cmlhp1ab* could be further affected by the gene deregulation at the systemic level, reaching a point in which the female parental function is costly to maintain, and therefore, MF development is favored. The latter might explain as well why the few FFs found in *Cmlhp1ab* were unable to set fruit; however, an alternative or additional explanation for this can be related to the direct role of CmLHP1 proteins in fruit development.

On the whole, we propose a model in which CmLHP1A and B act as positive regulators of female flower development. At the systemic level, LHP1 regulates hormone responses and plant architecture which, when unaltered, trigger the activation of a *CmACS11* development-dependent regulatory network at future FF buds. Once CmACS11 is switched on or off at the flower bud, CmLHP1A and B action might be required for regulating flower development, hormone homeostasis, and SDG expression in a sex-specific manner (Figure 6).

One of the main constraints when studying epigenomic regulators, such as LHP1, is the broad range of mechanisms they regulate, so discerning between direct or indirect effects related to a specific phenotype becomes tricky. Despite this limitation, we have shown that epigenomic regulators, such as LHP1, play a role in the repression of genes involved in plant development and is required for controlling the male:female ratio in monoecious melon. Finally, these results shed light on the molecular mechanisms by which GSD and, potentially, ESD control SDGs.

EXPERIMENTAL PROCEDURES

Phylogenetic analysis

We identified potential homologs of LHP1, CLF, and SWN proteins using PLAZA 4.0, an online source for plant comparative genomics (Van Bel et al., 2017). LHP1 belongs to homolog family HOM04D003850. Full-length protein sequences were retrieved for *Arabidopsis thaliana* (AT5G17690), *Arabidopsis lyrata* (AL6G28780), *Carica papaya* (Cpa.g.sc73.30), *Solanum lycopersicum* (Solyc01g 081500.2.1, Solyc10g024470.1.1), *Populus trichocarpa* (Potri.019G 044400.1, Potri.013G070400), *Zea mays* (GRMZM2G117100), and *O. sativa* (Os10g0324900). LHP1 protein sequences for cucurbits were extracted from the Cucurbits genomic database CuGenDB (Zheng et al., 2018) for *C. sativus* (CsaV3_3G009890.1, CsaV3_6G006350.1), *C. melo* (MELO3C006209, MELO3C022484, version V3.6.1), *Momordica charantia* (XP 022155759.1, XP 022147101.1), and *Citrullus lanatus* (Cla021326, Cla006977). Similarly to LHP1 homologs, CLF and SWN homolog sequences were retrieved from PLAZA, (Homolog family HOM04D001615). We re-annotated *CmCLF* and *CmSWN* genes using RNA-seq data from monoecious melon and comparing them with ESTs (expressed sequence tag) deposited in the FLAGdb++ interface. Genomic data, CDSs, and protein sequences can be found in Data S1.

For assessing phylogenetic relationships, we aligned full-length protein sequences using ClustalW. Phylogenetic trees were constructed through MEGA7 (http://www.megasoftware.net/index.html) based on the neighbor-joining method. Protein sequence alignment was visualized in Jalview (Waterhouse et al., 2009) and colored in terms of identity percentage.

Plant material and growth conditions

Monoecious melon (*C. melo*) cultivar charentais (*C. melo* L. subsp. *melo* var *cantalupensis*) was used as the parental control line for all the experiments. Germinated seeds were transferred to 10-L pots and placed in a glasshouse under long day conditions, at a temperature of 27°C during the day and 21°C during the night and under a relative humidity of 60%. EMS homozygous mutants and segregating populations were multiplied until the M3 generation and backcrossed to the parental line. The *Cmlhp1ab* double mutants were obtained from the self-pollination of the *Cmlhp1ab* sesquimutant (*Cmlhp1Aa/bb*).

TILLING approach

CmCLF, *CmSWN*, *CmLHP1A*, and *CmLHP1B* mutations were screened on an EMS-mutagenized seed collection consisting on 8000 M2 families. DNA isolation, 3D pooling, and mutation detection were performed as described in (Boualem et al., 2015). SENTINEL software was used for identification and annotation of the mutations (Clepet et al., 2021) and mutations were confirmed by Sanger sequencing.

Sexual phenotyping

Sexual transitions of 45-day-old plants of monoecious WT and *CmLHP1a*, *b*, and *ab* mutants were estimated based on the sex of flowers located at the L1 node of LBs (Figure 5i). We registered

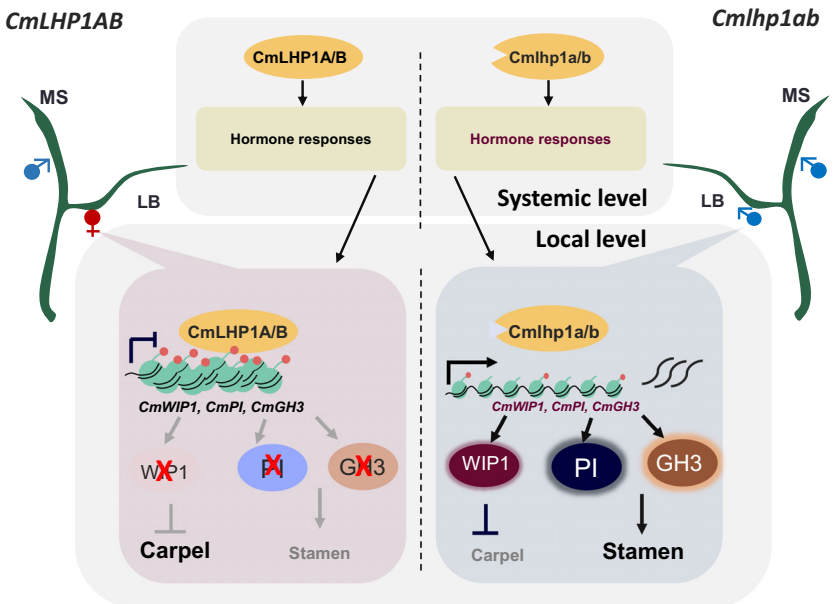

Figure 6. Proposed model for the roles of CmLHP1A and B in melon sex determination. At the systemic level, LHP1A and B are involved in the control of several biological processes such as hormone responses. At the local level, in the female flower, CmLHP1A and B negatively control the expression of genes involved in carpel abortion (i.e., *CmWIP1*), stamen development (e.g., *CmPI*), and hormone balance (*CmGH3*) by maintaining H3K27me27 levels at these loci. In *Cmlhp1ab* mutants, male-promoting genes display reduced levels of H3K27me3, thus favoring the development of male flowers over female. MS: main stem, LB: lateral branch. Gray and black arrows indicate inactivated and activated regulatory processes, respectively. Red colored text denotes deregulated (up and down) processes.

this for 170 L1 nodes for each phenotype, which corresponds to at least five plants of WT and *CmLHP1* single mutants and 15 *Cmlhp1ab* plants. Female-to-male transitions were quantitatively expressed as the 'ratio of masculinized branches', which corresponds to the number of L1 nodes bearing male flowers divided by the total number of branches registered.

RNA and RNA-seq library preparations

Total RNA was extracted from leaves using the Nucleospin RNA kit (Macherey–Nagel), according to the manufacturer's instructions. For RNA-seq analysis, libraries were synthetized using the NEBNext Ultrall Directional RNA library Preparation Kit (NEB) according to the manufacturer's instructions. Three biological replicates were generated for WT and *Cmlhp1ab* plants. Libraries were prepared using the NEBNext® Ultra™ II Directional RNA Library Prep Kit for Illumina; 76-bp single-read end sequencing was performed on a HiSeq 1500 device (Illumina).

Differential expression analysis

After library sequencing, adapters were removed with trimmomatic v0.38 using the following parameters: ILLUMINACLIP: TruSeq3-SE.fa:2:30:10, LEADING: 5, TRAILING: 5, MINLEN: 30. Reads were mapped on the v4.0 genome assembly of *C. melo* L (DHL92) using STAR with the following parameters: --sjdbOverhang 75 --outFilterType BySJout --outSAMtype BAM SortedByCoordinate --outFilterIntronMotifs RemoveNoncanonical. The read count matrix was obtained using featureCounts with the following parameters: -F GTF -t exon -g gene_id -T 8 -M -O -s 2 -Q 30. Differentially expressed genes were identified using R 3.5.1 (www.R-project.org) and the package DESeq2 ($P_{adj} < 0.05$).

Chromatin immunoprecipitation experiments

ChIP experiments were carried out as previously described for Arabidopsis plantlets (Ramirez-Prado et al., 2021), with minor modifications. Briefly, 1 g of fresh leaves was cross-linked in 1% (v/v) formaldehyde for 15 min. Cross-linking was quenched by adding glycine at a final concentration of 0.125 M for 5 mins. Samples were homogenized and nuclei were isolated and lysed. The buffer composition and a detailed explanation of chromatin preparation can be found in (Ramirez-Prado et al., 2021). Cross-linked melon chromatin was sonicated using a Covaris S220 (peak power: 175 W, 200 cycles per burst, duty factory: 20%) for 9 min. For H3K27me3 ChIP-seq, protein–DNA complexes were immunoprecipitated with anti-H3K27me3 (Millipore, ref. 07-449) antibodies overnight at 4°C with gentle shaking. Next, chromatin–antibody complexes were incubated with Dynabeads Protein A (Invitrogen, Ref. 100-02D) for 2 h. Beads were then washed twice for 5 min in Low Salt Wash Buffer (0.1% SDS, 1% Triton X-100, 20 mM Tris-HCl pH 8, 2 mM EDTA pH 8, 150 mM NaCl), twice for 5 min in High Salt Wash Buffer (0.1% SDS, 1% Triton X-100, 20 mM Tris-HCl pH 8, 2 mM EDTA pH 8, 500 mM NaCl), twice for 5 min in LiCl Wash Buffer (0.25 M LiCl, 1% NP-40, 1% sodium deoxycholate, 10 mM Tris-HCl pH 8, 1 mM EDTA pH 8), and twice in TE buffer (10 mM Tris-HCl pH 8, 1 mM EDTA pH 8). Immunoprecipitated DNA was eluted after a 15-min incubation at 65°C with 250 µl Elution Buffer (1% SDS, 0.1 M $NaHCO_3$). This step was repeated once for a total of two elutions. Chromatin was reverse cross-linked by adding 20 µl of 5 M NaCl and incubated overnight at 65°C. Reverse cross-linked DNA was then treated with RNase and proteinase K and extracted with phenol/chloroform/IAA. Next, DNA was precipitated with ethanol and 1 µl of GlycoBlue™ (ThermoFisher, Invitrogen, catalog number: AM9516) and incubated overnight at −20°C. The DNA pellet was then resuspended in 20 µl of nuclease-free water (Ambion) in a DNA low-bind tube. Next, 10 ng of immunoprecipitated or input DNA was used for ChIP-seq library construction using the NEB-Next Ultra II DNA Library Prep Kit for Illumina (New England Biolabs, catalog number: NEB #E7645S/L) according to the manufacturer's recommendations.

For the Pol II ChIP assay, we immunoprecipitated chromatin using anti-Pol II (AB_2732926) as previously explained for H3K27me3 ChIP. Before isolating protein–DNA complexes, we pre-incubated the Dynabeads Protein G (Invitrogen, 100-07D) with a bridging anti-mouse IgG (Active Motif, 53017) for 1 h at 4°C and gentle shaking. Dynabeads protein G plus bridging antibody coupled solution was then added to the sample. Bead washing and the following steps were performed as explained above for H3K27me3 ChIP-seq.

Computational analysis of ChIP-seq

After sequencing, adapters were removed from the obtained reads with trimmomatic v0.38, using the following parameters: ILLUMINACLIP: TruSeq3-SE.fa:2:30:10, LEADING: 5, TRAILING: 5, MINLEN: 30. Reads from all ChIP-seq experiments were mapped to the v4.0 genome assembly of *C. melo* L. (DHL92) with Bowtie2 v.2.3.5 and the ---very-sensitive setting. Reads with MAPQ $\leq$ 30 and PCR duplication were removed from mapped reads with samtools v1.9. Peaks were identified with MACS2 v2.2.7 with the command MACS2 callpeak --broad -t sample.bam -c Input.bam -g 7.8e8 -q 0.05 --extsize 150 --bw 500 -B -n --outdir. Peaks from each experiment were annotated using the v4.0 gene annotation of *C. melo* L (https://www.melonomics.net/) and bedtools v2.28.0 closest.

RPGC depth-normalized values of the read densities were computed over 20-bp bins with Deeptools v3.1.0 bamCoverage and used to draw the metaplots and heatmaps with Deeptools computeMatrix, plotHeatmap, and plotProfile. The normalized read densities were also used to generate co-occurrence plots over the TSSs of genes using R 3.5.1 (www.R-project.org) and the package ggplot2 v3.1.0 (www.github.com) with geom_bin2d (bins = 200).

Bigwig files were normalized with the S3norm method with default parameters and deposited at GitHub (https://github.com/guanjue/S3norm). MAnorm2_utils were used to prepare the input files for differential analysis. Then normBioCond, fitMeanVarCurve, diffTest, and the built-in function MAnorm2 were used to conduct the differential expression analysis. H3K27me3 peaks were annotated using the v4.0 annotation of *C. melo* L with bedtools v2.28.0 closest. For identifying hypermethylated and hypomethylated genes, we set a peak distance of $\pm$2 kb and an Ma cutoff value ($\log_2$(FC)) of 0.4.

qRT-PCR experiments

Female and male flowers from monoecious and *Cmlhp1ab* double mutants were sampled and sorted based on their node position (MS or proximal nodes from LBs). After sampling, flowers were further sorted by size and separated in different developmental stages. Male and female flowers from stage 7 (Bai et al., 2004) and 0.5-mm *Cmlhp1ab* flowers were used to assess gene expression. RNA was extracted using the Macherey-Nagel NucleoSpin RNA plus kit, according to the manufacturer's instructions. First strand cDNA was synthesized from 1 μg of RNA using the ImProm-II™ Reverse Transcription System from Promega, following the manufacturer's instructions. Products were amplified and fluorescence signals were acquired with a Bio-Rad CFX384 Touch™ Real-Time PCR Detection System. The specificity of amplification products was determined by melting curves. *CmACT2* was used as internal control for signal normalization. The relative quantification was performed following the $2^{-\Delta\Delta Ct}$ method. Data were obtained from duplicates of three biological replicates. Sequences of primers can be found in Data S4.

ACKNOWLEDGMENTS

This work was supported by the European Research Council (ERC-SEXYPARTH, 341076), the ANR (EPISEX, ANR-17-CE20-0019), and the LabEx Saclay Plant Sciences (SPS) (ANR-10-LABX-40-SPS).

AUTHOR CONTRIBUTIONS

AbB and MB devised the research project. NRG, AbB, and MB designed the methodology. NR performed the majority of experiments, characterization of mutants, and data mining and led the writing of the article. CT, MH, CS, and RC performed the TILLING approach. RBC contributed with some ChIP-seq experiments. JA, SS, and DMM performed the bioinformatic analysis. CD and AdB supervised the project and contributed to the generation of plant material. JR, DL, CR, AbB, and MB analyzed the data and complemented the writing.

CONFLICT OF INTEREST

The authors declare that they have no conflicts of interest related to this research.

DATA AVAILABILITY STATEMENT

The data described in this article have been deposited with NIH/NCBI as GEO dataset GSE180386.

SUPPORTING INFORMATION

Additional Supporting Information may be found in the online version of this article.

Figure S1. CmCLF and CmSWN phylogenetic relationships, expression profiles, and gene body structures.

Figure S2. Gene expression profile of *CmLHP1A* and *B*.

Figure S3. *Cmlhp1a* splicing mutation.

Figure S4. *Cmlhp1ab* mutants display up- and downregulation of genes involved in an arsenal of biological processes.

Figure S5. Spearman correlation heatmap between monoecious WT and *Cmlhp1ab* H3K27me3 ChIP-seq biological replicates from leaves.

Figure S6. Gene expression deregulation in *Cmlhp1ab* is associated with H3K27me3-mediated regulation.

Figure S7. Boxplot showing H3K27me3 levels of deregulated genes in *Cmlhp1ab*.

Figure S8. Gene expression and H3K27me3 profiles of *CmWIP1*, *CmACS11*, and *CmACS7* in WT and *Cmlhp1ab* flowers.

Data S1. Genes up- and downregulated in *Cmlhp1ab* double mutants.

Data S2. H3K27me3-marked genes and differentially methylated genes in *Cmlhp1ab* double mutants.

Data S3. FF- and MF-specific genes hyper- and hypomethylated in *Cmlhp1ab* double mutants.

Data S4. Primers used for qPCR experiments.

REFERENCES

Akagi, T., Henry, I.M., Kawai, T., Comai, L. & Tao, R. (2016) Epigenetic regulation of the sex determination gene megi in polyploid persimmon. *The Plant Cell*, **28**, 2905–2915. Available from: http://www.plantcell.org/lookup/doi/ https://doi.org/10.1105/tpc.16.00532

Ariel, F., Jegu, T., Latrasse, D., Romero-Barrios, N., Christ, A., Benhamed, M. & Crespi, M. (2016) Noncoding transcription by alternative RNA polymerases dynamically regulates an auxin-driven chromatin loop. *Molecular Cell*, **55**, 383–396.

Bai, S.L., Peng, Y.B., Cui, J.X., Gu, H.T., Xu, L.Y., Li, Y.Q. *et al.* (2004) Developmental analyses reveal early arrests of the spore-bearing parts of reproductive organs in unisexual flowers of cucumber (*Cucumis sativus L.*). *Planta*, **220**, 230–240.

Bai, S.N. & Xu, Z.H. (2013) Unisexual cucumber flowers, sex and sex differentiation. *International Review of Cell and Molecular Biology*, **304**, 1–55.

Barrero, J.M., González-Bayón, R., del Pozo, J.C., Ponce, M.R. & Micol, J.L. (2007) INCURVATA2 encodes the catalytic subunit of DNA polymerase α and interacts with genes involved in chromatin-mediated cellular

memory in *Arabidopsis thaliana*. *The Plant Cell*, **19**, 2822–2838. Available from: http://www.plantcell.org/content/19/9/2822.abstract

Berry, S., Rosa, S., Howard, M., Bühler, M. & Dean, C. (2017) Disruption of an RNA-binding hinge region abolishes LHP1-mediated epigenetic repression. *Genes & Development*, **31**, 2115–2120.

Boualem, A., Fergany, M., Fernandez, R., Troadec, C., Martin, A., Morin, H. *et al.* (2008) A conserved mutation in an ethylene biosynthesis enzyme leads to andromonoecy in melons. *Science*, **321**, 836–838.

Boualem, A., Troadec, C., Camps, C., Lemhemdi, A., Morin, H., Sari, M.-A. *et al.* (2015) A cucurbit androecy gene reveals how unisexual flowers develop and dioecy emerges. *Science*, **350**, 688–691. Available from: http://www.sciencemag.org/content/350/6261/688.abstract

Chanvivattana, Y., Bishopp, A., Schubert, D., Stock, C., Moon, Y.H., Sung, Z.R. *et al.* (2004) Interaction of Polycomb-group proteins controlling flowering in Arabidopsis. *Development*, **131**, 5263–5276.

Chen, D.H., Huang, Y., Ruan, Y. & Shen, W.H. (2016) The evolutionary landscape of PRC1 core components in green lineage. *Planta*, **243**, 825–846.

Chuck, G., Meeley, R., Irish, E., Sakai, H. & Hake, S. (2007) The maize tasselseed4 microRNA controls sex determination and meristem cell fate by targeting Tasselseed6/indeterminate spikelet1. *Nature Genetics*, **39**(12), 1517–1521. Available from: http://dx.doi.org/https://doi.org/10.1038/ng.2007.20

Clepet, C., Devani, R.S., Boumlik, R., Hao, Y., Morin, H., Marcel, F., *et al.* (2021) The miR166-SlHB15A regulatory module controls ovule development and parthenocarpic fruit set under adverse temperatures in tomato. *Molecular Plant.*, **14**(7), 1185–1198. Available from: https://doi.org/10.1016/j.molp.2021.05.005

Coen, E.S. & Meyerowitz, E.M. (1991) The war of the whorls: genetic interactions controlling flower development. *Nature*, **353**, 31–37.

Cui, H. & Benfey, P.N. (2009) Interplay between SCARECROW, GA and LIKE HETEROCHROMATIN PROTEIN 1 in ground tissue patterning in the Arabidopsis root. *The Plant Journal*, **58**, 1016–1027. Available from: https://doi.org/https://doi.org/10.1111/j.1365-313X.2009.03839.x

Dahmani-Mardas, F., Troadec, C., Boualem, A., Lévêque, S., Alsadon, A.A., Aldoss, A.A. *et al.* (2010) Engineering melon plants with improved fruit shelf life using the TILLING approach. *PLoS One*, **5**(12), e15776.

Derkacheva, M. & Hennig, L. (2014) Variations on a theme: polycomb group proteins in plants. *Journal of Experimental Botany*, **65**, 2769–2784.

Derkacheva, M., Steinbach, Y., Wildhaber, T., Mozgová, I., Mahrez, W., Nanni, P. *et al.* (2013) Arabidopsis MSI1 connects LHP1 to PRC2 complexes. *EMBO Journal*, **32**, 2073–2085.

Diggle, P.K., Stilio, V.S.D., Gschwend, A.R., Golenberg, E.M., Moore, R.C., Russell, J.R.W. *et al.* (2011) Multiple developmental processes underlie sex differentiation in angiosperms. *Trends in Genetics*, **27**, 368–376.

Exner, V., Aichinger, E., Shu, H., Wildhaber, T., Alfarano, P. & Caflisch, A. *et al.* (2009) The chromodomain of LIKE HETEROCHROMATIN PROTEIN 1 Is Essential for H3K27me3 Binding and function during Arabidopsis development. *PLoS One*, **4**, e5335. Available from: https://journals.plos.org/plosone/article?id=10.1371/journal.pone.0005335

Feng, J. & Lu, J. (2017) LHP1 could act as an activator and a repressor of transcription in plants. *Frontiers in Plant Science*, **8**, 1–7. Available from: http://journal.frontiersin.org/article/https://doi.org/10.3389/fpls.2017.02041/full

Galun, E. (1959) The role of auxins in the sex expression of the cucumber. *Physiologia Plantarum*, **12**(1), 48–61.

Gaudin, V., Libault, M., Pouteau, S., Juul, T., Zhao, G., Lefebvre, D. *et al.* (2001) Mutations in LIKE HETEROCHROMATIN PROTEIN 1 affect flowering time and plant architecture in Arabidopsis. *Development*, **128**, 4847–4858. Available from: http://dev.biologists.org/content/128/23/4847.abstract

Goodrich, J., Puangsomlee, P., Martin, M., Long, D., Meyerowitz, E.M. & Coupland, G. (1997) A Polycomb-group gene regulates homeotic gene expression in Arabidopsis. *Nature*, **386**, 44–51. Available from: http://dx.doi.org/https://doi.org/10.1038/386044a0

Grossniklaus, U., Vielle-Calzada, J.-P., Hoeppner, M.A. & Gagliano, W.B. (1998) Maternal control of embryogenesis by MEDEA, a polycomb group gene in arabidopsis. *Science*, **280**, 446–450. Available from: http://www.sciencemag.org/content/280/5362/446.abstract

Grumet, R. & Taft, J. (2011) Sex expression in Cucurbits. *Genet. Genomics Breed. Cucurbits*, 353–375.

Harkess, A. & Leebens-Mack, J. (2016) A century of sex determination in flowering plants. *Journal of Heredity*, **108**, 69–77. Available from: https://doi.org/https://doi.org/10.1093/jhered/esw060

He, C., Chen, X., Huang, H. & Xu, L. (2012) Reprogramming of H3K27me3 is critical for acquisition of pluripotency from cultured Arabidopsis tissues. *PLoS Genetics*, **8**, e1002911. Available from: https://pubmed.ncbi.nlm.nih.gov/22927830

Hennig, L. & Derkacheva, M. (2009) Diversity of polycomb group complexes in plants: same rules, different players? *Trends in Genetics*, **25**, 414–423. Available from: http://www.sciencedirect.com/science/article/pii/S0168952509001498

Hu, Y., Shen, Y., Conde e Silva, N. & Zhou, D.X. (2011) The role of histone methylation and H2A.Z occupancy during rapid activation of ethylene responsive genes. *PLoS One*, **6**, e28224. Available from: https://doi.org/https://doi.org/10.1371/journal.pone.0028224

Huang, Y., Chen, D., Liu, B., Shen, W. & Ruan, Y. (2017) Conservation and diversification of polycomb repressive complex 2 (PRC2) proteins in the green lineage. *Briefings in Functional Genomics*, **16**(2), 106–119.

Irish, E.E. & Nelson, T. (1989) Sex determination in monoecious and dioecious plants. *The Plant Cell*, **1**, 737.

Köhler, C., Hennig, L., Spillane, C., Pien, S., Gruissem, W. & Grossniklaus, U. (2003) The Polycomb-group protein MEDEA regulates seed development by controlling expression of the MADS-box gene PHERES1. *Genes & Development*, **17**, 1540–1553.

Korpelainen, H. (1998) Labile sex expression in plants. *Biological Reviews*, **73**, 157–180.

Kotake, T., Takada, S., Nakahigashi, K., Ohto, M. & Goto, K. (2003) Arabidopsis TERMINAL FLOWER 2 gene encodes a heterochromatin protein 1 homolog and represses both FLOWERING LOCUS T to regulate flowering time and several floral homeotic genes. *Plant and Cell Physiology*, **44**, 555–564. Available from: https://doi.org/https://doi.org/10.1093/pcp/pcg091

Lafos, M., Kroll, P., Hohenstatt, M.L., Thorpe, F.L., Clarenz, O. & Schubert, D. (2011) Dynamic regulation of H3K27 trimethylation during arabidopsis differentiation. *PLoS Genetics*, **7**, e1002040. Available from: https://doi.org/https://doi.org/10.1371/journal.pgen.1002040

Lai, Y.S., Shen, D., Zhang, W. *et al.* (2018) Temperature and photoperiod changes affect cucumber sex expression by different epigenetic regulations. *BMC Plant Biology*, **18**, 1–13.

Lai, Y.S., Zhang, X., Zhang, W. *et al.* (2017) The association of changes in DNA methylation with temperature-dependent sex determination in cucumber. *Journal of Experimental Botany*, **68**, 2899–2912.

Larsson, A.S., Landberg, K. & Meeks-Wagner, D.R. (1998) The TERMINAL FLOWER2 (TFL2) gene controls the reproductive transition and meristem identity in *Arabidopsis thaliana*. *Genetics*, **149**, 597–605.

Latrasse, D., Germann, S., Houba-Hérin, N., et al. (2011) Control of flowering and cell fate by LIF2, an RNA binding partner of the polycomb complex component LHP1. *PLoS One*, **6**, e16592. Available from: https://doi.org/https://doi.org/10.1371/journal.pone.0016592

Latrasse, D., Rodriguez-Granados, N.Y., Veluchamy, A., Mariappan, K.G., Bevilacqua, C., Crapart, N. *et al.* (2017) The quest for epigenetic regulation underlying unisexual flower development in Cucumis melo. *Epigenetics and Chromatin*, **10**, 1–17.

Li, S.-F., Lv, C.-C., Lan, L.-N., Jiang, K.-L., Zhang, Y.-L., Li, N., Deng, C.-L. & Gao, W.-J. (2021) DNA methylation is involved in sexual differentiation and sex chromosome evolution in the dioecious plant garden asparagus. *Horticulture Research*, **8**. Available from: http://dx.doi.org/https://doi.org/10.1038/s41438-021-00633-9

Li, Z., Li, B., Liu, J. *et al.* (2016) transcription factors AS1 and AS2 interact with LHP1 to repress to repress KNOX genes in Arabidopsis. *Journal of Integrative Plant Biology*, **58**, 959–970.

Libault, M., Tessadori, F., Germann, S., Snijder, B., Fransz, P. & Gaudin, V. (2005) The Arabidopsis LHP1 protein is a component of euchromatin. *Planta*, **222**, 910–925.

Liu, C., Xi, W., Shen, L., Tan, C. & Yu, H. (2009) Regulation of floral patterning by flowering time genes. *Developmental Cell*, **16**, 711–722. Available from: http://www.sciencedirect.com/science/article/pii/S1534580709001324

Liu, X., Zhou, S., Wang, W., Ye, Y., Zhao, Y.U., Xu, Q. *et al.* (2015) Regulation of histone methylation and reprogramming of gene expression in

the rice inflorescence meristem. *The Plant Cell*, **27**, 1428–1444. Available from: https://pubmed.ncbi.nlm.nih.gov/25957386

Ma, W.J. & Pannell, J.R. (2016) Sex determination: separate sexes are a double turnoff in melons. *Current Biology*, **26**(4), R171–R174. Available from: http://dx.doi.org/https://doi.org/10.1016/j.cub.2015.12.026

Margueron, R. & Reinberg, D. (2011) The Polycomb complex PRC2 and its mark in life. *Nature*, **469**, 343–349.

Martin, A., Troadec, C., Boualem, A., Rajab, M., Fernandez, R., Morin, H., Pitrat, M., Dogimont, C. & Bendahmane, A. (2009) A transposon-induced epigenetic change leads to sex determination in melon. *Nature*, **461**, 1135–1138. Available from: http://dx.doi.org/https://doi.org/10.1038/nature08498

Mylne, J.S., Barrett, L., Tessadori, F. *et al.* (2006) LHP1, the Arabidopsis homologue of HETEROCHROMATIN PROTEIN1, is required for epigenetic silencing of FLC. *Proceedings of the National Academy of Sciences of the United States of America*, **103**, 5012–5017.

Olmo, I.Del, López-González, L., Martín-Trillo, M.M., Martínez-Zapater, J.M., Piñeiro, M. & Jarillo, J.A. (2010) EARLY IN SHORT DAYS 7 (ESD7) encodes the catalytic subunit of DNA polymerase epsilon and is required for flowering repression through a mechanism involving epigenetic gene silencing. *The Plant Journal*, **61**, 623–636. Available from: https://doi.org/https://doi.org/10.1111/j.1365-313X.2009.04093.x

Pannell, J.R. (2017) Plant sex determination. *Current Biology*, **27**, R191–R197. Available from: http://dx.doi.org/https://doi.org/10.1016/j.cub.2017.01.052

Parihar, V., Arya, D., Walia, A., *et al.* (2019) Functional characterization of LIKE HETEROCHROMATIN PROTEIN 1 in the moss Physcomitrella patens: Its conserved protein interactions in land plants. *The Plant Journal*, **97**, 221–239. Available from: https://doi.org/https://doi.org/10.1111/tpj.14182

Pawełkowicz, M., Pryszcz, L., Skarzyńska, A., Wóycicki, R.K. & Posyniak, K. (2019) Comparative transcriptome analysis reveals new molecular pathways for cucumber genes related to sex determination. *Plant Reproduction*, **32**, 193–216. Available from: https://doi.org/https://doi.org/10.1007/s00497-019-00362-z

Pawełkowicz, M.E., Skarzyńska, A., Pląder, W. & Przybecki, Z. (2019) Genetic and molecular bases of cucumber (*Cucumis sativus L.*) sex determination. *Molecular Breeding*, **39**, 50. Available from: https://doi.org/https://doi.org/10.1007/s11032-019-0959-6

Pfent, C., Pobursky, K.J., Sather, D.N. & Golenberg, E.M. (2005) Characterization of SpAPETALA3 and SpPISTILLATA, B class floral identity genes in Spinacia oleracea, and their relationship to sexual dimorphism. *Development Genes and Evolution*, **215**, 132–142.

Piacentini, L., Fanti, L., Berloco, M., Perrini, B. & Pimpinelli, S. (2003) Heterochromatin protein 1 (HP1) is associated with induced gene expression in Drosophila euchromatin. *Journal of Cell Biology*, **161**, 707–714. Available from: https://pubmed.ncbi.nlm.nih.gov/12756231

Qiu, Y., Liu, S.L. & Adams, K.L. (2017) Concerted divergence after gene duplication in polycomb repressive complexes. *Plant Physiology*, **174**, 1192–1204.

Ramirez-Prado, J.S., Latrasse, D. & Benhamed, M. (2021) Histone modification ChIP-seq on *Arabidopsis thaliana* Plantlets. *Bio-Protocol*, **11**, e4211. Available from: https://doi.org/https://doi.org/10.21769/BioProtoc.4211

Ramirez-Prado, J.S., Latrasse, D., Rodriguez-Granados, N.Y. *et al.* (2019) The Polycomb protein LHP1 regulates *Arabidopsis thaliana* stress responses through the repression of the MYC2-dependent branch of immunity. *The Plant Journal*, **100**, 1118–1131.

Rattan, P. & Kumar, S. (2016) Sex expression in cucurbits special reference to cucumber and melon. In: Pessarakli, M. (Ed.) *Handbook of cucurbits: growth, cultural practices, and physiology*. Boca Raton, FL: CRC Press, pp. 201–210.

Rizzardi, K., Landberg, K., Nilsson, L., Ljung, K. & Sundås-Larsson, A. (2011) TFL2/LHP1 is involved in auxin biosynthesis through positive regulation of YUCCA genes. *The Plant Journal*, **65**, 897–906.

Rodriguez-Granados, N.Y., Lemhemdi, A., Choucha, F.A., Latrasse, D., Benhamed, M., Boualem, A. *et al.* (2017) Sex determination in Cucumis. In: Grumet, R., Katzir, N. & Garcia-Mas, J. (Eds.) *Genetics and genomics of Cucurbitaceae. Plant genetics and genomics: Crops and models*. Cham: Springer, pp. 307–319. Available from: https://doi.org/10.1007/7397_2016_32

Sather, D.N., Jovanovic, M. & Golenberg, E.M. (2010) Functional analysis of B and C class floral organ genes in spinach demonstrates their role in sexual dimorphism. *BMC Plant Biology*, **10**:46.

Schubert, D., Primavesi, L., Bishopp, A., Roberts, G., Doonan, J., Jenuwein, T. *et al.* (2006) Silencing by plant Polycomb-group genes requires dispersed trimethylation of histone H3 at lysine 27. *EMBO Journal*, **25**, 4638–4649.

Takahashi, H., Suge, H. & Saito, T. (1980) Sex expression as affected by N6-benzylaminopurine in staminate inflorescence of Luffa cylindrica. *Plant and Cell Physiology*, **21**(4), 525–536. Available from: https://doi.org/https://doi.org/10.1093/oxfordjournals.pcp.a076028

Tanurdzic, M. & Banks, J.A. (2004) Sex-determining mechanisms in land plants. *The Plant Cell*, **16**, S61–S71 Available from: http://www.plantcell.org/content/16/suppl_1/S61.short

Turck, F., Roudier, F., Farrona, S., Martin-Magniette, M.-L., Guillaume, E., Buisine, N. *et al.* (2007) Arabidopsis TFL2/LHP1 specifically associates with genes marked by trimethylation of histone H3 lysine 27. *PLoS Genetics*, **3**, e86.

Van Bel, M., Diels, T., Vancaester, E., Kreft, L., Botzki, A., Van de Peer, Y., Coppens, F. & Van de Poele, K. (2017) PLAZA 4.0: An integrative resource for functional, evolutionary and comparative plant genomics. *Nucleic Acids Research*, **46**(D1), D1190–D1196.

Veluchamy, A., Jégu, T., Ariel, F., Latrasse, D., Mariappan, K.G., Kim, S.-K. *et al.* (2016) LHP1 regulates H3K27me3 spreading and shapes the three-dimensional conformation of the arabidopsis genome. *PLoS One*, **11**, e0158936.

Vyskot, B., Araya, A., Veuskens, J., Negrutiu, I. & Mouras, A. (1993) DNA methylation of sex chromosomes in a dioecious plant, Melandrium Album. *Molecular & General Genetics*, **239**, 219–224.

Waterhouse, A.M., Procter, J.B., Martin, D.M.A., Clamp, M. & Barton, G.J. (2009) Jalview Version 2—a multiple sequence alignment editor and analysis workbench. *Bioinformatics*, **25**, 1189–1191. Available from: https://doi.org/https://doi.org/10.1093/bioinformatics/btp033

Wei, W., Tao, J.-J., Chen, H.-W., Li, Q.-T., Zhang, W.-K., Ma, B., Lin, Q., Zhang, J.-S. & Chen, S.-Y. (2017) A histone code reader and a transcriptional activator interact to regulate genes for salt tolerance. *Plant Physiology*, **175**, 1304–1320. Available from: http://www.plantphysiol.org/content/175/3/1304.abstract

Yang, H.W., Akagi, T., Kawakatsu, T. & Tao, R. (2019) Gene networks orchestrated by MeGI: a single-factor mechanism underlying sex determination in persimmon. *The Plant Journal*, **98**, 97–111.

Zheng, Y., Wu, S., Bai, Y., *et al.* (2018) Cucurbit Genomics Database (CuGenDB): a central portal for comparative and functional genomics of cucurbit crops. *Nucleic Acids Research*, **47**(D1), D1128–D1136.